

MINISTÉRIO DA CIÊNCIA E TECNOLOGIA



CBPF

CENTRO BRASILEIRO DE PESQUISAS FÍSICAS

Notas de Física

CBPF-NF-008/88

ELECTRONIC STRUCTURE AND ISOMER SHIFTS OF Sn HALIDES

by

Joyce Terra and Diana Guertzburger

ABSTRACT

The all-electron first-principles Discrete Variational method was employed to study the electronic structure of SnF_4 , SnCl_4 , SnBr_4 and SnI_4 . Values of the electronic density at the Sn nucleus were derived and related to ^{119}Sn Isomer Shifts to obtain the nuclear constant $\Delta\langle r^2 \rangle$. Differences in values of $\rho(0)$ are discussed in terms of the chemical bonding between Sn and halogen atoms.

Key-words: Isomer shifts; Electronic structure.

I INTRODUCTION

The Isomer Shift δ , as measured by Mössbauer Spectroscopy, depends both on a nuclear factor and an electronic factor⁽¹⁾. The latter, $\Delta\rho(0)$, is the difference between the electronic density at the nucleus in the probe atom in two different environments and reflects the difference in the chemical interactions of this atom. For this reason, the Isomer Shift can give important information about the electronic structure and chemical bonding in compounds and alloys, and a wide variety of applications have been made in Chemistry and solid state Physics. However, the qualitative and quantitative interpretation of this information requires the knowledge of the nuclear factor, which is the relative variation of the nuclear radius, $\Delta R/R$, in the Mössbauer transition.

In the case of the most widely studied Mössbauer probe, ^{57}Fe , the nuclear constant $\Delta R/R$ has already been reasonably well established through a large number of experimental and theoretical efforts⁽¹⁾⁻⁽³⁾. For the less studied Mössbauer isotope ^{119}Sn , a number of determinations of $\Delta R/R$ have been made⁽⁴⁾⁻⁽²¹⁾, but unfortunately there is a significant disagreement between the results derived. So far, the majority of the proposed values for $\Delta R/R$ have been obtained in two manners. It may be obtained either by combining the difference in Isomer Shift for two distinct chemical states of Sn with the calculated value of the charge density at the nucleus for each of the states⁽⁴⁾⁻⁽¹⁷⁾, or it can be derived by combining a change in Isomer Shift with an estimate, by some other technique (as for example internal

conversion), of the corresponding change in the electron density at the nucleus and a calculation of the electron density for one state of Sn⁽¹⁸⁾⁻⁽²¹⁾.

All the calculations of $\rho(0)$ have been made considering the Sn atom as free⁽⁴⁾⁻⁽²¹⁾, (with a very recent exception which we refer to later), mainly due to the fact that Sn is a considerably larger atom than Fe, thus constituting a bigger challenge for electronic structure calculations. However, Mössbauer experiments on matrix - isolated Sn have shown that even rare-gas matrix effects on $\rho(0)$ might be of the order of $\sim 5\%$ ⁽¹⁵⁾. Accordingly, the extensive contradiction between the values of $\Delta R/R$ estimated may be ascribed to the use of atomic wave functions, which is unsuitable because no proper account is taken of the neighborhood effects on the probe atom.

In this work we present a determination of $\Delta R/R$ for ¹¹⁹Sn by means of first - principles all-electrons self - consistent electronic structure calculations on four compounds of Sn, namely SnF₄, SnCl₄, SnBr₄ and SnI₄, employing the Discrete Variational (DV) LCAO Molecular Orbitals method^{(22),(23)} in the local density approximation. Local density methods have been employed to study isomer shifts⁽²⁴⁾, and the DV method was used to investigate isomer shifts in inorganic compounds⁽²⁵⁾, as well as metals and alloys⁽²⁶⁾. The choice of these compounds was based on the fact that they are solids with a well defined crystallography, besides spanning a wide range of values of δ . Values of the electronic density at the Sn nucleus were derived for these compounds, and were combined with the experimental δ values to obtain the nuclear factor. Differences in

$\rho(0)$ obtained are discussed in the light of the different factors related to the chemical bonds.

A very recent attempt to calculate $\rho(0)$ for these compounds of Sn has been reported in the literature⁽²⁷⁾. The authors employed both the Hartree Fock LCAO Molecular Orbitals method with the pseudopotential approximation for the core, and the Multiple Scattering -X α method with the muffin-tin approximation for the molecular potential. Here we analyse briefly the differences and similarities of our method and the methods in that work, and compare the results.

This paper is organized as follows: in section II we describe the main features of the theoretical method and calculation procedure. In part III we present and discuss the results obtained. In part IV we summarize our main conclusions.

II THEORETICAL METHOD

A - Discrete Variational Method (DVM)

We employed the Discrete Variational Method (DVM) in the local density approximation as has been described in detail elsewhere^{(22),(23),(28)}, to perform electronic structure calculations of clusters representing the solids. The fundamental problem is to solve the set of one-electron equations

$$(H - \epsilon_i) \psi_i(\vec{r}) = 0 \quad (1)$$

where the one-electron Hamiltonian is given (in Hartrees) by:

$$H = -\frac{1}{2} \nabla^2 + V_{\text{coul}}(\rho) + V_{x\alpha}(\rho) \quad (2)$$

where the local exchange potential $V_{x\alpha}$ is^{(29), (30)}

$$V_{x\alpha}(\rho) = -3\alpha \left[\frac{3}{8\pi} \rho(\vec{r}) \right]^{1/3} \quad (3)$$

with $\alpha = 2/3$. The Coulomb potential V_{coul} includes nuclear and electronic contributions and the electronic density $\rho(\vec{r})$ at point \vec{r} is taken as a sum over the molecular orbitals ψ_i with occupation n_i

$$\rho(\vec{r}) = \sum_i n_i |\psi_i(\vec{r})|^2 \quad (4)$$

The one-electron molecular wave functions are expanded on a basis of symmetrized numerical atomic orbitals χ_j^s (LCAO approximation)

$$\psi_i(\vec{r}) = \sum_j c_j^i \chi_j^s(\vec{r}) \quad (5)$$

The coefficients that define the molecular orbitals $\psi_i(\vec{r})$ and their one-electron energies ϵ_i are found by solving the secular equations

$$([\mathbf{H}] - [\mathbf{E}][\mathbf{S}])[\mathbf{C}] = 0 \quad (6)$$

where the matrix elements are numerical integrals on a three-dimensional grid. The integrations are performed in three dimensions with the pseudo-random Diophantine Method⁽²²⁾. For the calculation of hyperfine interactions, however, additional caution is required in the numerical procedures at the core region of the probe atom, where precision of the matrix elements is difficult to achieve due to the large oscillations of the wave functions; for this reason, a special integration scheme was used inside a sphere containing the core electrons of the probe atom, involving a systematic polynomial integration in three dimensions⁽²⁸⁾.

An approximation to $\rho(\vec{r})$ is employed to define the Hamiltonian in Eq. 2⁽²³⁾. A Mulliken-type population analysis is performed for the atoms in the cluster and the charge density is approximately defined as

$$\rho(\vec{r}) \cong \sum_{vnl} f_{nl}^v |R_{nl}(r_v)|^2 \quad (7)$$

where $R_{nl}(r_v)$ is the radial part of atomic orbital $\chi_v(\vec{r}) = R_{nl}(r_v) Y_{\ell}^m(\hat{r}_v)$ centered on site v , and f_{nl}^v is the Mulliken-type population of this orbital. Iterations are made until the populations achieve self-consistency. All electrons are included in the calculations, and the core is completely relaxed.

In the DV method, the crystal is simulated by an embedding scheme, where we considered numerical atomic potentials at a number of sites surrounding the cluster. Since the chemical environment of the solid is thus considered, the main question is the definition of the clusters, which must

be chosen as the most representative of the crystal, that is to say, they must provide an adequate representation of the neighborhood felt by the tin atom. For SnCl_4 , SnBr_4 and SnI_4 , we considered the tetrahedral clusters present in the crystals^{(31),(32)}. Mössbauer spectroscopy measurements on the Ar matrix-isolated molecules SnX_4 ($X = \text{Cl}, \text{Br}, \text{I}$) show that, within the experimental error, the isomer shifts of Sn in these species are identical to the crystals⁽³³⁾. This result indicates that our choice of clusters in these cases is very reasonable. In the solids, the tetrahedral coordination around the Sn is slightly distorted⁽³¹⁾⁽³²⁾; however, this distortion was not considered in our calculations, and T_d symmetry was adopted. On the other hand, the same experiments on matrix-isolated tin(IV) fluoride⁽³³⁾ showed a marked difference in the Mössbauer parameters, as compared to the crystalline solid. Indeed, this solid has a layered structure⁽³⁴⁾, which results in a strong tetragonal distortion of the octahedral coordination of the six fluorine atoms surrounding the Sn, the axial Sn-F interatomic distances being shorter than the equatorial distances. It is this distortion which gives rise to the observed Quadrupole Splitting in crystalline SnF_4 ⁽³⁵⁾. In the tetragonal (D_{4h}) cluster $[\text{SnF}_6]^{-x}$ considered in our calculation, this distortion was taken into account, with interatomic distances as in the crystal. The charge ($-x$) of the cluster was determined self-consistently, as described later. In Fig. 1 we show the two types of clusters and in Table 1 are given the interatomic distances.

B - Mössbauer Isomer Shift

The isomer shift δ , as defined in a Mössbauer spectroscopy measurement, formally can be written as^{(1), (35)}

$$\delta = \alpha \Delta \rho_e(0) \quad (8)$$

$$\text{with } \alpha = \frac{2}{3} \pi Z e^2 \Delta \langle r^2 \rangle S'(Z) \quad \text{or} \quad \alpha = \frac{4}{5} \pi Z e^2 R^2 (\Delta R/R) S'(Z) \quad (9)$$

$$\text{and } \Delta \rho_e(0) = \left[\sum_i n_i |\psi_i(0)|_A^2 - \sum_j n_j |\psi_j(0)|_S^2 \right] \quad (10)$$

where $\Delta \langle r^2 \rangle$ is the difference in the mean square nuclear radius, whereas $\Delta R/R$ is the change in the nuclear charge radius for a uniform charge distribution of $R = 1.2 \times A^{1/3}$ fm, between the excited and ground states in the Mössbauer nuclear transition (23.8 KeV for ^{119}Sn). The chemical term is the difference between the electron charge density at the nuclear site related to the absorber \underline{A} and the source \underline{S} , the summations being over the molecular orbitals ψ_i occupied by n_i electrons (see Eq. 4); $S'(Z)$ is the correction factor (2.306 for ^{119}Sn ⁽⁶⁾) if relativistic effects are not taken into account in the calculation of the wave functions.

We have derived the nuclear factors $\Delta \langle r^2 \rangle$ (or $\Delta R/R$) in Eq. 9, by combining experimental measurements of δ in the four crystals studied, with the corresponding calculated values of $\Delta \rho_e(0)$, as in Eq. 10. The correction for relativistic effects employed can be considered suitable. Indeed, it has been demonstrated that differences in $\Delta \rho_e(0)$ for ions in different

oxidation states are well described by non-relativistic charge density differences multiplied by the linear factor $S'(Z)^{(36)}$. Since our study is essentially comparative, the same reasoning applies here, and the errors introduced by the use of non-relativistic wave functions and a constant $S'(Z)$ are not very significant. Only the molecular orbitals belonging to the totally symmetric representation will have finite probability at the origin.

III RESULTS AND DISCUSSION

A - Some details of the calculations

As described in Section II, our calculations involve an expansion of the one-electron molecular functions on a basis of numerical self-consistent local-density atomic orbitals. As this basis is necessarily incomplete, it must be chosen carefully. Winkler et al. ⁽²⁷⁾ pointed out to be fact that truncated basis sets in LCAO methods may constitute a severe limitation to realistic estimates of isomer shifts, due to lack of flexibility. However, in the present calculations this limitation was largely bypassed, by the following procedure: at the end of each convergence of the self-consistent potential, a Mulliken-type population analysis is performed, and the populations obtained used to define atomic charges and configurations for the Sn and halogen atoms. For these configurations, new self-consistent atomic calculations are performed to obtain new atomic orbitals for the basis. This procedure is repeated

until the configuration of the basis atomic orbitals is approximately the same as that of the "atoms" in the cluster. This adaptation of the atomic wave functions to the actual situation in the compound compensates to a large extent the limitation on the number of terms in the LCAO expansion.

For the Sn atom, the virtual orbitals 6s and 6p were added to the basis, to augment the variational freedom. To further increase the quality of the valence basis functions, a potential well was included in the atomic potential (in the atomic calculations) so as to somewhat contract the diffuse exterior orbitals, creating functions more consistent with the actual situation in the solid. This well was defined with the same characteristics for Sn in all four clusters, so as not to impair the comparison among the compounds, and it was chosen carefully so as not to alter significantly the shape of the valence orbitals of the atom, a feature found to be important for a good description of the isomer shifts.

No empty orbitals were included for the halogen atoms Cl, Br and I, and no well was considered necessary. In fact, test calculations using potential wells on the halogen atoms showed that even small distortions of the valence functions of the larger atoms (Br and I) may affect critically the value of $\rho(0)$ at the Sn site, due to the contribution to $\rho(0)$ of the neighbor atoms diffuse functions. For the F atom, which acquired a much larger negative charge during the self-consistent process, as compared to the other three halogens, a more rigid potential well was necessary, to achieve convergence and to obtain more contracted valence functions, thus getting more meaningful re-

sults. This feature has been noticed before in DVM calculations for the ionic compounds CaF_2 , SrF_2 and BaF_2 ⁽³⁷⁾. Part of the reason for this characteristic is that large negative charges lead to very diffuse orbitals, and for these the Mulliken populations represent badly the atomic charges, and consequently, so do the self-consistent cluster potentials based on them (see Eq. 7).

As described in section II, an embedding scheme was employed, with the inclusion of several shells of numerical atomic densities centered on the crystal sites exterior to the cluster, thus creating an embedding potential. Again, the atomic densities for the outer atoms were obtained by atomic local-density self-consistent calculations, for the same configurations as in the cluster. It was gratifying to observe that all three sets of atomic configurations (cluster, basis and exterior atoms) do, indeed, converge to the same point, making us confident that a consistent picture was obtained for the electronic structure of the crystals.

As mentioned in Section II, all electrons were included in the calculations. Although the differences in $\rho(0)$ for the 1s, 2s and 3s orbitals of Sn in the different clusters may be considered negligible, the inclusion of all orbitals in the self-consistent calculations assures that all effects of core relaxation due to rearrangement of the valence electrons are properly taken into account.

B - Electronic structure

In Table II are given the self-consistent Mulliken populations and the charges for all four clusters investigated. The charge of -1.5 on the fluorine cluster was obtained self-consistently, in order that the charges on the atoms approximately obey the stoichiometry of the compound SnF_4 . At the end of each convergence, the total number of electrons was modified to satisfy the stoichiometry, using the charge on Sn as a guide.

The positive charge on Sn decreases from F to I, as expected from the increase in covalency of the Sn-X bond. There is a marked difference between the charge on Sn in the $[\text{SnF}_6]^{-1.5}$ cluster and the Sn charge on the other clusters. This is consistent with the marked difference in electronegativity between F and the other halogens. But even for this most ionic case, the charges are very far from the formal +4 for Sn and -1 for F. The decrease of the positive charge on Sn along the series corresponds to an increase in the occupation of the valence orbitals 5s and 5p. In the case of SnI_4 , the 6p orbital was also significantly populated. In the case of $[\text{SnF}_6]^{-1.5}$, there is a marked depletion of the 5s and 5p orbitals, corresponding to a charge transfer from the Sn atom to the F atoms, which is more pronounced for the equatorial fluorines.

In Fig. 2 are shown the higher energy one-electron energy levels of the clusters (eigenvalues ϵ_i of Eq. 1), where the dashed lines mean the first empty level.

For $[\text{SnF}_6]^{-1.5}$, the lower energy set, constituted by mo-

lecular orbitals $8a_{1g}$ to $2b_{2g}$, forms the 4d band of Sn. The next group formed by $9a_{1g}$, $5a_{2u}$ and $5e_u$ is predominantly of F(2s) character, both axial and equatorial. The orbitals $4b_{1g}$, $10a_{1g}$ and, in particular, $11a_{1g}$, are the ones that show more admixture between the Sn and F orbitals, with the Sn 4d orbitals participating in the first two forming bonds with the F(2s), and the Sn 5s orbital participating in the latter. Bonding between the Sn 5p orbital and F is seen in the next orbitals $6e_u$ and $6a_{2u}$. Finally, the set from $5b_{1g}$ to the last occupied orbital $4e_g$ forms the 2p band of fluorine, having negligible contribution of the Sn orbitals. The overall characteristic of the electronic structure of $[\text{SnF}_6]^{-1.5}$ is of a predominantly ionic compound, with little mixture between the Sn and F orbitals.

The lower energy set of orbitals for SnCl_4 , as depicted in Fig. 2, is formed by $9t_2$ and $3e$, which are constituted primarily of 4d functions of Sn. The $8a_1$ and $10t_2$ orbitals, which are next in energy, show some admixture with the Sn 5s ($8a_1$), 4d and 5p ($10t_2$) orbitals, but are predominantly of Cl 3s character. $9a_1$ shows a large degree of mixture between Sn 5s and Cl 3s, and in $11t_2$ the mixture between Sn 5p, Cl 3s and Cl 3p is also large. The last three occupied levels are essentially of Cl 3p character.

The characteristics of the electronic structure of SnCl_4 are essentially repeated in SnBr_4 and SnI_4 . For those two clusters, the first set of levels ($15t_2$ and $6e$ for SnBr_4 and $21t_2$ and $9e$ for SnI_4) are of Sn 4d character. The next four orbitals ($11a_1$, $16t_2$, $12a_1$ and $17t_2$ for SnBr_4 and $14a_1$, $22t_2$, $15a_1$ and $23t_2$ for

SnI_4) are of covalent nature, presenting considerable mixture of Sn 5s, 4d and 5p orbitals with the valence orbitals of the halogen atom. Finally, the highest occupied three orbitals of e , t_2 and t_1 symmetry are essentially constituted of the valence p orbitals of the halogen.

One may observe that the energies of the valence orbitals of the clusters of T_d symmetry increase with increasing atomic number of the halogen.

C - Isomer Shifts

Table III to Table VI show individual orbital contributions to $\rho(0)$ for the Sn halides, for the orbitals associated primarily to the 4s level of Sn ("shallow core") and for the valence orbitals of appropriate symmetry. Differences between values of $\rho(0)$ for the core orbitals of Sn are negligible. For each of the orbitals considered, are also given the energy and the electronic distribution in terms of Mulliken populations. It is seen that the increase in $\rho(0)$ along the series of halides is related to an increase in 5s occupation of valence orbitals. This is consistent with the increase in covalent character from SnF_4 to SnI_4 , with the consequent decrease of the positive charge on Sn.

The total values of $\rho(0)$ are correlated to the experimental Isomer Shifts in Fig. 3. As both $\rho(0)$ and the measured values of δ increase along the series, we obtain a positive calibration constant in Eq. 8, with the following values for the nuclear constants of ^{119}Sn :

$$\Delta \langle r^2 \rangle = + 9.21 \times 10^{-3} \text{ fm}^2$$

or
$$\Delta R/R = + 2.20 \times 10^{-4} \quad \text{with } R = 1.2 \text{ xA}^{1/3} \text{ fm}$$

Due mainly to basis functions dependence, we estimate crudely an error of approximately $\pm 10\%$ for these values.

The considerable distance between the point for $[\text{SnF}_6]^{-1.5}$ from the other halides is consistent with the much more accentuated ionic character of the fluoride.

It is customary, in the literature, to describe the causes of differences in $\rho(0)$ in different compounds as due mainly to two effects, identified as "potential distortion" and "overlap distortion", both concepts deriving from atomic models. The former is associated to changes in $\rho(0)$ due to changes in the potential around the Mössbauer atom, and the latter is related to orthogonality effects between the core orbitals and valence orbitals on neighbor atoms. In our calculations, these effects are all taken into account simultaneously, and in a self-consistent manner. In particular, the inclusion of all core electrons in the calculations is important to include "overlap distortion" effects in an appropriate manner.

A larger number of earlier attempts to obtain $\Delta R/R$ for ^{119}Sn were made employing crude atomic models, resulting in values of $\Delta R/R$ ranging from -2.5 to $+3.6 \times 10^{-4}$ ⁽²¹⁾. The recently reported first-principles calculations of Winkler et al. ⁽²⁷⁾ also resulted in a very good correlation between $\rho(0)$ and δ for Sn^{IV} halides. However, the LCAO Gaussian expansion method employed

by the authors had the rather severe limitation of the pseudo-potential approximation for the core, and poor flexibility of the basis set, which the authors attempted to circumvent in a rather "ad hoc" manner. The Multiple Scattering Method, which was also employed, does not have these limitations, although its use is restricted to compact clusters; however, the muffin-tin approximation to the cluster potential adopted in this method is rather poor, and it has been shown⁽³⁸⁾ that calculated values of $\rho(0)$ are extremely sensitive to the muffin-tin radii chosen. The values of $\Delta R/R$ obtained by these authors, however, do not differ significantly from our value of $\Delta R/R = 2.20 \times 10^{-4}$. In fact, they obtain 2.00×10^{-4} and 1.80×10^{-4} with the pseudo-potential LCAO method, and 1.92×10^{-4} with the Multiple Scattering. The similarity between these results obtained with three non-empirical quantum chemistry methods so different in nature is very gratifying, and gives us confidence that modern electronic structure methods are indeed a reliable tool to study problems of hyperfine interactions in such complex compounds as Sn halides.

IV CONCLUSIONS

We have performed first-principles all-electron electronic structure calculations for Sn^{IV} halides, and derived a value of 2.20×10^{-4} for the nuclear parameter $\Delta R/R$ of ^{119}Sn . A good correlation between $\rho(0)$ and δ was obtained with the DV method. The use of configuration-adapted numerical atomic orbitals in the LCAO basis, crystal embedding and inclusion of core electrons

are a definite improvement over conventional LCAO methods. However, the problem of limited basis sets still remains, and results are consequently somewhat sensitive to the basis functions. The use of numerical self-consistent atomic basis functions optimized to the physical problem at hand offers very interesting possibilities, to be explored further.

ACKNOWLEDGMENTS

This work was supported by the Conselho Nacional de Desenvolvimento Científico e Tecnológico (CNPq) and by the National Science Foundation, grant No. INT 83-12863.

FIGURE CAPTIONS

Figure 1: Clusters representing Sn halide crystals.

Figure 2: Valence one-electron energy levels scheme for Sn clusters.

Figure 3: Isomer shift $\times \rho(0)$ correlation for Sn halides.

- a) Experimental values from Reference (35). Related to SnO_2 .

TABLE CAPTIONS

Table I: Crystallographic data for Sn halides^(a)

(a) See references (31), (32) and (34).

(b) Average distance

Table II: Charges and Mulliken populations for the Sn clusters.

Table III: Energy, charge distribution and $\rho(0)$ of molecular orbitals of symmetry a_{1g} for $[\text{SnF}_6]^{-1.5}$

Table IV: Energy, charge distribution and $\rho(0)$ of molecular orbitals of symmetry a_1 for SnCl_4 .

Table V: Energy, charge distribution and $\rho(0)$ of molecular orbitals of symmetry a_1 for SnBr_4 .

Table VI: Energy, charge distribution and $\rho(0)$ of molecular orbitals of symmetry a_1 for SnI_4 .

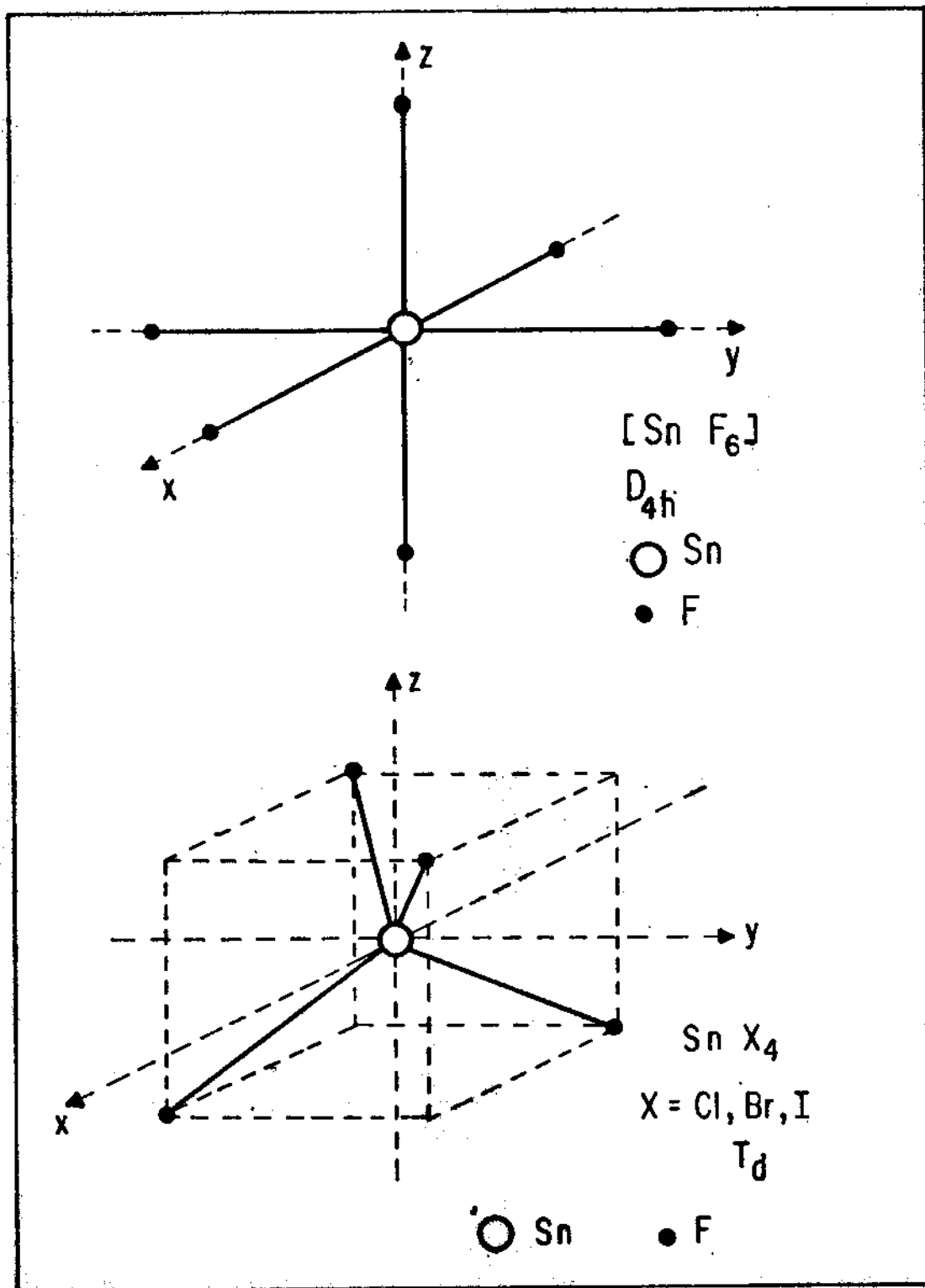


Fig. 1

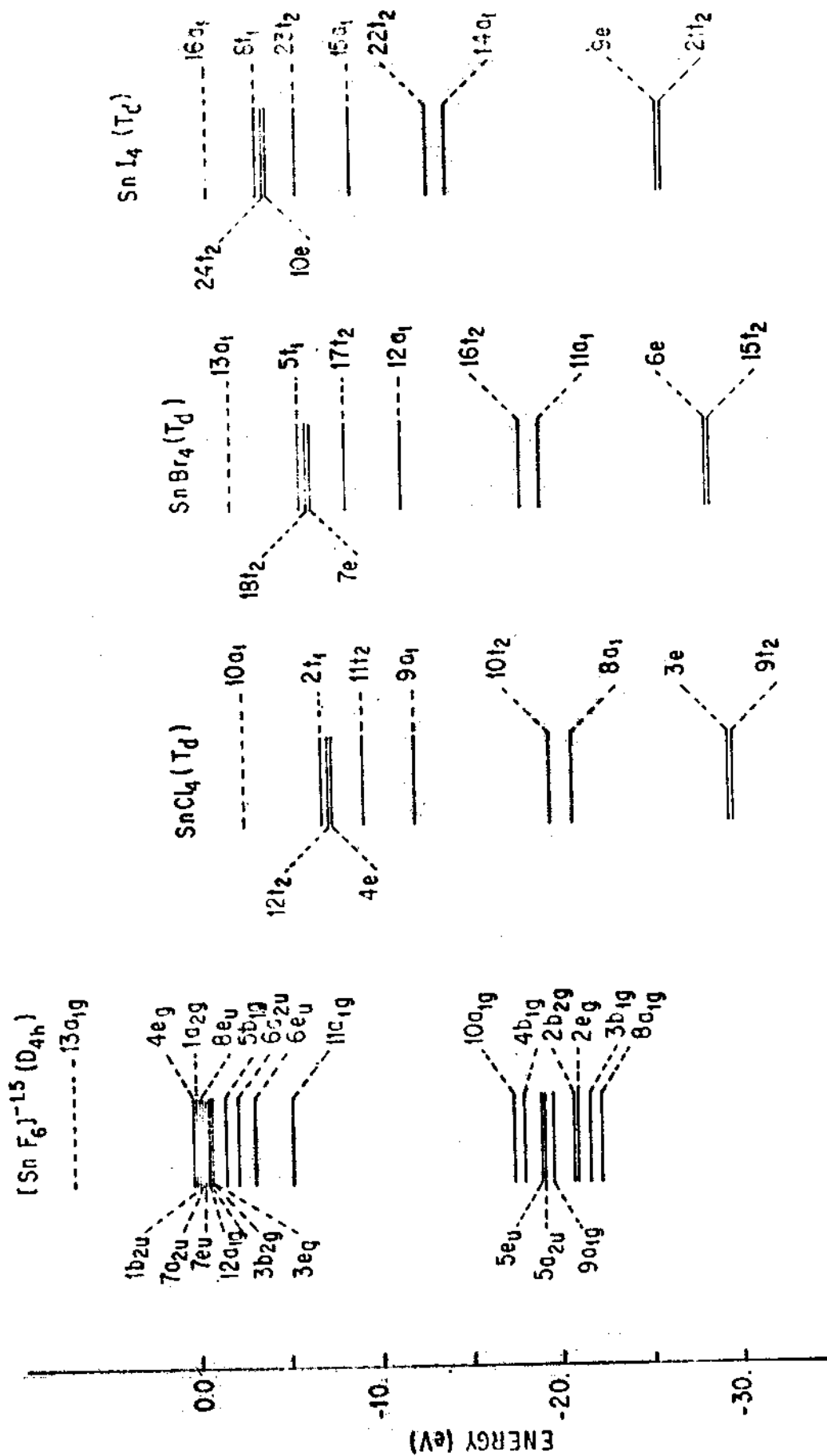


Fig. 2

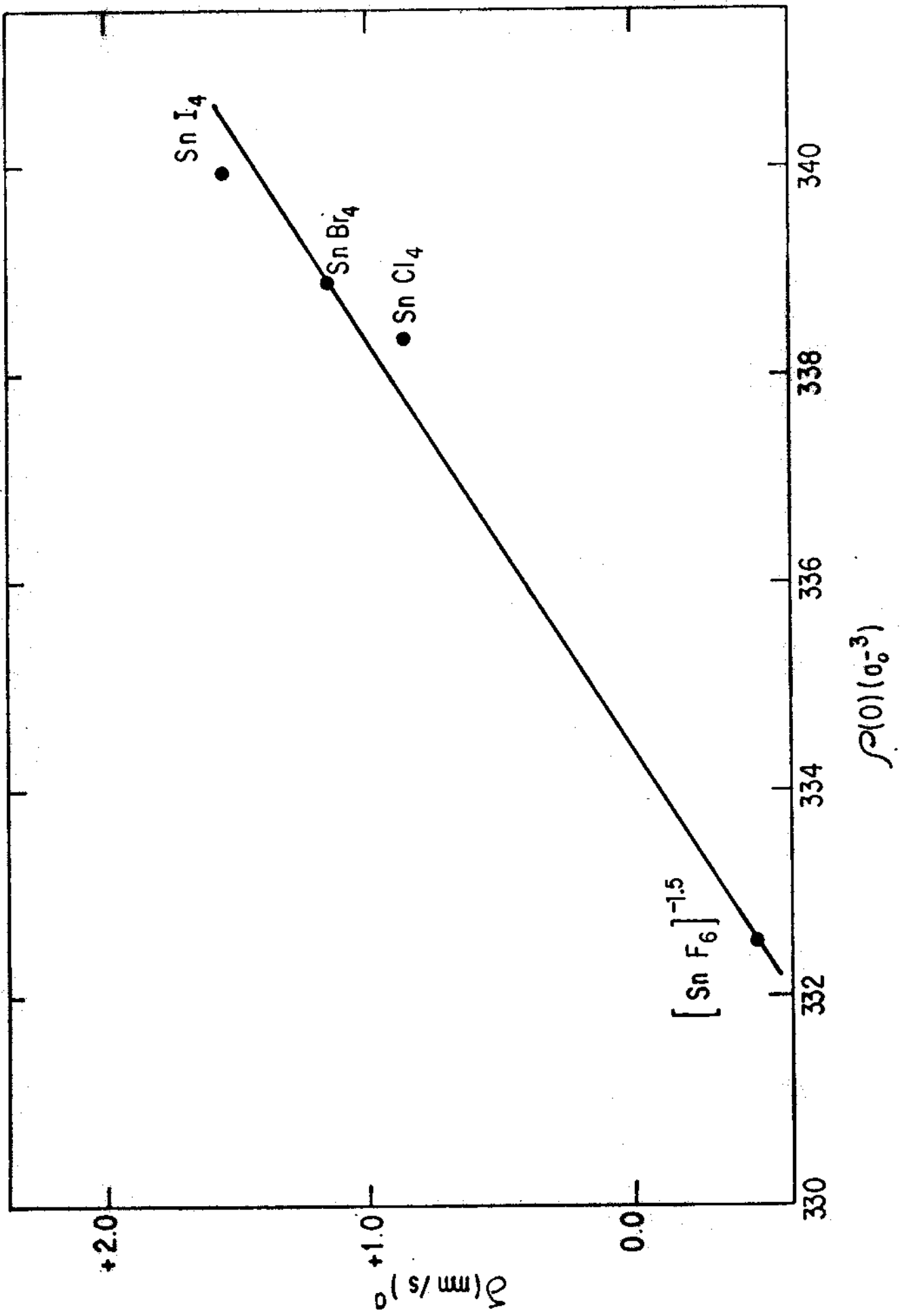


Fig. 3

TABLE I

	$[\text{SnF}_6]^{-x}$	SnCl_4	SnBr_4	SnI_4
Crystallographic structure	Tetragonal	Monoclinic	Monoclinic	Cubic
Sn-X distance (\AA)	$\left\{ \begin{array}{l} 2.02 \text{ (eq.)} \\ 1.88 \text{ (ax.)} \end{array} \right.$	2.26 ^(b)	2.46 ^(b)	2.69 ^(b)
X-Sn-X angle	-	102.25 ⁰	109.25 ⁰	-
Lattice Parameters (\AA)	$\left\{ \begin{array}{l} 4.04 \\ 4.04 \\ 7.93 \end{array} \right.$	$\left\{ \begin{array}{l} 9.80 \\ 6.75 \\ 9.98 \end{array} \right.$	$\left\{ \begin{array}{l} 10.59 \\ 7.10 \\ 10.66 \end{array} \right.$	$\left\{ \begin{array}{l} 12.26 \\ 12.26 \\ 12.26 \end{array} \right.$

TABLE II

	$[\text{SnF}_6]^{-1.5}$	SnCl_4	SnBr_4	SnI_4				
Sn	4s	1.998	1.993	1.994	1.997			
	4p	5.997	5.996	5.996	5.997			
	4d	9.992	9.994	9.995	5.996			
	5s	0.578	1.141	1.300	1.506			
	5p	0.470	1.077	1.305	1.568			
	6s	0.004	0.015	0.016	0.019			
	6p	0.049	0.050	0.070	0.238			
	Charge: +2.909	+1.730	+1.319	+0.676				
halogen	2s (eq.)	1.976	2p	5.999	3p	5.999	4s	1.998
	2p (eq.)	5.804	3s	1.970	3d	9.999	4p	5.999
	2s (ax.)	1.975	3p	5.463	4s	1.969	4d	9.999
	2p (ax.)	5.668			4p	5.361	5s	1.959
							5p	5.213
	Charge: -0.780 (eq.) -0.644 (ax.)	-0.432		-0.329		-0.169		

TABLE III

<u>Orbital</u>	<u>Energy</u> (in eV)	<u>Charge distribution</u> (in % of one electron)	$\rho(0)$ (in a_0^{-3})
$7a_{1g}$	-117.06	$\sim 100\%$ Sn(4s)	314.37
$8a_{1g}$	-22.26	74.7Sn(4d _{z²}), 2.0F _{eq} (2s), 21.8F _{ax} (2s), 1.3F _{ax} (2p)	0.12
$9a_{1g}$	-19.54	2.2Sn(5s), 1.1Sn(4d _{z²}), 76.9F _{eq} (2s), 19.2F _{ax} (2s)	1.89
$10a_{1g}$	-17.44	26.3Sn(4d _{z²}), 20.6F _{eq} (2s), 52.6F _{ax} (2s)	0.15
$11a_{1g}$	-5.18	23.9Sn(5s), 3.9F _{eq} (2s), 51.4F _{eq} (2p); 5.6F _{ax} (2s), 14.4F _{ax} (2p)	15.39
$12a_{1g}$	-0.57	4.4Sn(4d _{z²}), 30.3F _{eq} (2p), 64.1F _{ax} (2p)	0.62

Total $\rho(0)$: 332.55

TABLE IV

<u>Orbital</u>	<u>Energy</u> (in eV)	<u>Charge distribution</u> (in % of one electron)	$\frac{\rho(0)}{(\text{in } a_0^{-3})}$
$7a_1$	-125.71	$\sim 100\%$ Sn(4s)	314.26
$8a_1$	-20.83	8.4 Sn(5s), 85.1 Cl(3s), 5.7 Cl(3p)	5.39
$9a_1$	-12.16	39.8 Sn(5s), 22.7 Cl(3s), 36.5 Cl(3p)	18.71

Total $\rho(0)$:

338.36

TABLE V

<u>Orbital</u>	<u>Energy</u> (in eV)	<u>Charge distribution</u> (in % of one electron)	$\frac{\rho(0)}{(\text{in } a_0^{-3})}$
9a ₁	-124.87	~ 100% Sn(4s)	314.26
10a ₁	-66.39	~ 100% Br(3d)	0.0
11a ₁	-19.40	9.4 Sn(5s), 86.0 Br(4s), 3.9 Br(4p)	4.97
12a ₁	-11.70	45.9 Sn(5s), 22.7 Br(4s), 30.3 Br(4p)	19.72

Total $\rho(0)$: 338.95

TABLE VI

<u>Orbital</u>	<u>Energy</u> (in eV)	<u>Charge distribution</u> (in % of one electron)	<u>$\rho(0)$</u> (in a_0^{-3})
11a ₁	-122.57	~ 100% Sn(4s)	314.27
12a ₁	-120.78	~ 100% I(4p)	0.0
13a ₁	-49.23	~ 100% I(4d)	0.0
14a ₁	-14.64	18.4Sn(5s), 77.0I(5s), 4.1I(5p)	7.02
15a ₁	-9.25	48.6 Sn(5s), 30.3I(5s), 19.9I(5p)	18.63

Total $\rho(0)$: 339.93

REFERENCES

- (1) see, for example, "Mössbauer Isomer Shifts", ed. G.K. Shenoy and F.E. Wagner, North Holland, Amsterdam (1978).
- (2) D. Guenzburger, D.M. Esquivel and J. Danon, Phys. Rev. B18, 4561 (1978).
- (3) W.C. Neuwpoort, D. Post and P.Th. van Duijnen, Phys. Rev. B17, 91 (1978).
- (4) A.J. Boyle, St. P. Bunbury and C. Edwards, Proc. Phys. Soc. London. 79, 416 (1962).
- (5) V.I. Goldanskii, G.M. Gorodinskii, S.V. Karyagin, L.A. Koritko, L.M. Karizhavskii, E.F. Makarov, I.P. Suzdalev and V.V. Khrapov, Proc. Acad. Sci. URRS, Phys. Chem. Sect. 147, 766 (1962).
- (6) D.A. Shirley, Rev. Mod. Phys. 36, 339 (1964).
- (7) M. Cordey-Hayes, J. Inorg. Nucl. Chem. 26, 915 (1964).
- (8) I.B. Bersuker, V.I. Goldanskii and E.F. Makarov, Sov. Phys. JETP 22, 485 (1966).
- (9) S.L. Ruby, G.M. Kalvius, G.B. Beard and R.E. Snyder, Phys. Rev. 159, 239 (1967).
- (10) J.K. Lees and P.A. Flinn, J. Chem. Phys. 48, 882 (1968).
- (11) N.N. Greenwood, P.G. Perkins and D.H. Wall, Phys. Lett. 28A, 339 (1968).
- (12) J. DeVooght, P.M. Gielen and S. Lejeune, J. Organometal. Chem. 21, 333 (1970).
- (13) H. Micklitz and P.H. Barret, Phys. Rev. B5, 1704 (1972).
- (14) E. Antonak, Phys. Stat. Sol. (b) 79, 605 (1977).
- (15) H. Micklitz, Hyp. Int. 3, 135 (1977).
- (16) E. Antoncik, Phys. Rev. B23, 6524 (1981).

- (17) E. Antoncik, *Hyp. Int.* 11, 265 (1981).
- (18) J.P. Bocquet, Y.Y. Chu, O.C. Kistner, M.L. Perlman and G.T. Emery, *Phys. Rev. Lett.* 17, 809 (1966).
- (19) G.T. Emery and M.L. Perlman, *Phys. Rev.* B1, 3885 (1970).
- (20) G.M. Rothberg, S. Guimard and N. Benczer-Koller, *Phys. Rev.* B1, 136 (1970).
- (21) H. Muramatsu, T. Miura, H. Nokahara, M. Fujioka and E. Tanaka, *Hyp. Int.* 20, 305 (1984).
- (22) D.E. Ellis, *Int. J. Quantum Chem.* S2, 35 (1968); D.E. Ellis and G.S. Painter, *Phys. Rev.* B2, 2887 (1970).
- (23) A. Rosén, D.E. Ellis, H. Adachi and F.W. Averill, *J. Chem. Phys.* 85, 3629 (1976).
- (24) D. Guenzburger, "Calculations of Hyperfine Interactions in transition metal compounds in the local density approximation", in "Local Density Approximations in Quantum Chemistry and Solid State Physics", ed. J.P. Dahl and J. Avery, Plenum Press, New York (1984), p. 573.
- (25) D. Guenzburger and D.E. Ellis, *Phys. Rev.* B22, 4203 (1980); D. Guenzburger, D.E. Ellis, P.A. Montano, G.K. Shenoy, S.K. Malik, D.G. Hinks, P. Vaishnava and C.W. Kimball, *Phys. Rev.* B32, 4398 (1985).
- (26) D. Guenzburger and D.E. Ellis, *Phys. Rev.* B31, 93 (1985); D.E. Ellis and D. Guenzburger, *Phys. Rev.* B31, 1514 (1985).
- (27) W. Winkler, R. Vetter and E. Hartmann, *Chem. Phys.* 114, 347 (1987).
- (28) A.H. Stroud, "Approximate calculation of Multiple Integrals", Prentice-Hall, Englewood Cliffs, N.J., (1971).

- (29) J.C. Slater, "The Self-consistent Field for Molecules and Solids", vol. 4 of "Quantum Theory of Molecules and Solids", McGraw-Hill, N. York (1974).
- (30) W.Kohn and L.J. Sham, Phys. Rev. 140, A 1133 (1965); R. Gaspar, Acta Phys. Acad. Sci. Hung., 3, 263 (1954).
- (31) Von P. Brand and H. Sackmann, Z. Anorg. Allg. Chem. 321, 262 (1963).
- (32) F.Meller and I. Fankuchen, Acta Cryst. 8, 343 (1955).
- (33) A. Schichl, F.J. Litterst, H. Micklitz, J.P. Devort and J.M. Friedt, Chem. Phys. 20, 371 (1970).
- (34) A.F. Wells, "Structural Inorganic Chemistry", Clarendon Press, Oxford, (1984), p.425.
- (35) N.N. Greenwood and T.C. Gibb, "Mössbauer Spectroscopy" Chapman and Hall, London (1971), p.390.
- (36) J.V. Mallow, A.J. Freeman and J.P. Desclaux, Phys. Rev. B13, 1884 (1976).
- (37) N.C. Amaral, B. Maffeo and D. Guenzburger, Physica Status Solidi (b) 117, 141 (1983).
- (38) M.L. de Siqueira, S. Larsson and J.W.D. Connolly, J. Phys. Chem. Solids, 36, 1419 (1975).